RESEARCH PAPER

Liquid–liquid micro-dispersion in a double-pore T-shaped microfluidic device

**K. Wang · Y. C. Lu · J. H. Xu · J. Tan ·
G. S. Luo**

Abstract For further understanding the dispersion process in the T-shaped microfluidic device, a double-pore T-shaped microchannel was designed and tested with octane/water system to form monodispersed plugs and droplets in this work. The liquid–liquid two-phase flow patterns were investigated and it was found that only short plugs, relative length $L/w < 1.4$, were produced. Additionally, the droplets flow was realized at phase ratios (F_C/F_D) just higher than 0.5, which is much smaller than that in the single-pore T-shaped microchannels. A repulsed effect between the initial droplets was observed in the droplet formation process and the periodic fluctuation flow of the dispersed phase was discussed by analyzing the resistances. Besides, the effect of the two-phase flow rates on the plug length and the droplet diameter was investigated. Considering the mutual effect of the initial droplets and the equilibrium between the shearing force with the interfacial tension, phase ratio and Ca number were introduced into the semi-empirical models to present the plug and droplet sizes at different operating conditions.

List of symbols

Ca	Capillary number
d	droplet diameter (mm)
d_{av}	average droplet size (mm)
d_p	diameter of the pore (mm)
d_w	initial droplets width (mm)

F_C	continuous phase flow rate (μL/min)
F_D	dispersed phase flow rate (μL/min)
F_P	pressure between the initial droplets
F_S	shearing force of the cross-flow
L_{av}	average length of the plugs (mm)
l_p	length of the pore (mm)
P_D	pressure in the dispersed fluid inlet (Pa)
P_C	pressure at the junction in the continuous fluid (Pa)
$R_{p,HP+S}$	flow resistance (m^{-3})
u_C	velocity of the cross flow (m/s)
V_D	dispersed phase flow rate through a pore (μL/min)
w	width of the channel (mm)

Greek letters

γ	interface tension (N/m)
Δp_f	pressure difference caused by the flow resistance (Pa)
Δp_i	pressure impetus of the dispersed fluid (Pa)
Δp_{Y-L}	pressure difference caused by the interfacial tension (Pa)
δ	standard deviation of droplet size (mm)
μ_C	viscosity of continuous phase (Pa s)
μ_D	viscosity of the dispersed phase (Pa s)
σ	polydispersity index (%)

K. Wang · Y. C. Lu · J. H. Xu · J. Tan · G. S. Luo (✉)
The State Key Lab of Chemical Engineering,
Department of Chemical Engineering,
Tsinghua University, Beijing 100084, China
e-mail: gsluo@tsinghua.edu.cn

1 Introduction

Liquid–liquid micro-dispersed emulsion systems have received great attention in recent years for their extensive applications in chemical reaction (deMello 2003), bioassays (Song et al. 2006), separation (Kralj et al. 2005), material production (Shui et al. 2007). There are many advantages for

micro-dispersion systems and one of them is the small dispersed size (Joanicot et al. 2005). Precise control of droplet size and polydispersity is demanded in many important potential applications and some methods have been established to produce emulsions with narrow size distribution (Günther et al. 2006; Lambrich et al. 2005). In the past decade, microfluidic devices have been developed quickly. Monodispersed droplets have been successfully prepared in those devices, such as T-shaped (Nisisako et al. 2002; Tice et al. 2004; van der Graaf et al. 2005), co-flowing (Chu et al. 2007a; Chu et al. 2007b) and hydrodynamic flow focusing microchannels (Anna et al. 2003; Xu and Nakajima 2004; Wang et al. 2007), with polydispersity index less than 5% (Christopher et al. 2007). By controlling the channel structure and the wetting properties the two-phase flow patterns and the droplet size can be easily controlled at different operating conditions (Xu et al. 2006b; Tan et al. 2008).

In our previous work, monodispersed droplets with diameters ranging from 50 to 500 μm were prepared in a capillary based T-shaped PMMA microchannels and two kinds of flow patterns, plugs flow and droplets flow, were formed at different phase ratios. (Xu et al. 2006a). By changing the variety and concentration of surfactant, the interfacial tension and the wetting property varied, disordered or ordered two-phase flow patterns could be controlled in the same channel and the effect of contact angle on the two-phase flow was investigated (Xu et al. 2006b). Additionally, it was found that the droplet size decreases with the increasing of continuous phase flow rate and viscosity, and the droplet size is determined by the Capillary number Ca. Furthermore, the T-shaped microchannels have been used in the production of monodispersed silica spheres (Chen et al. 2008) and microcapsules (Gong et al. 2007).

For broader applications, more complicated structures were designed in the T-shaped devices (Geerken et al. 2007; Zheng et al. 2004; Song et al. 2003). One of them is the micro-pores dispersion devices. The research work on the droplet formation process from large amount of pores was firstly reported by Nakajima et al. (Sugiura et al. 2002a, b) and they did a lot of researches on the bulk preparation of emulsions (Kobayashi et al. 2003, 2004, 2005). In this work, a new kind of T-shaped microfluidic device with only double pores at the junction was developed and tested by a liquid–liquid dispersion system. With this simple device, we tried to further understand the fundamental of cross-flowing dispersion process in T-shaped micro devices, especially for the dispersion phenomena and the dispersion rules. Two-phase flow patterns were dependent first on the flow rates of continuous phase and dispersed phase. Then, the new phenomena of the dispersion process were discussed. Finally, semi-empirical equations of plugs flow and droplets flow were established

to represent the relation between the operation conditions and dispersed scales.

2 Experimental

2.1 Device and method

The double-pore T-shaped microdevice was fabricated on a polymethyl methacrylate (PMMA) chip (3 mm in thickness) with end mill. After fabrication, the chip was sealed with another PMMA plate (1 mm in thickness) and cured at 105°C using high-pressure thermal sealing techniques. In Fig. 1a the broad lines represent the configuration of the microchannel and the thin lines shows the scale. The straight channel is 0.72 mm wide × 0.46 mm high and the diameter of two micro pores is 0.15 mm with a depth of 0.49 mm. The two pores were placed on the top of the oil inlet. Fig. 1b is a stereograph of the microchannel with transparent channel walls.

The flow rates of the two phases were controlled by two microsyringe pumps with two gastight microsyringes, respectively. N-octane was used as the dispersed phase and deionized water with 1.5%wt sodium dodecyl sulfate (SDS, C_{MC} 0.25%wt) was used as the continuous phase. The crossflowing rupture technique was used to form stable emulsion in the microchannel. The experimental temperature was controlled at 20°C (±2°C) in this work. Considering the modification effect of the surfactant on the wetting properties of the channel wall, the continuous phase was first pumped into the channel and 10 min later the dispersed phase was pumped in.

2.2 Visualization and analysis

Experiments were carried out on a microscope with high-speed CCD video camera and the images were recorded at a frequency of 250 images/s. The length of oil plugs (l_{av}) or the diameter of oil droplets (d_{av}) in the channel was measured from microscope images. After changing any of the flow parameters, we allowed at least 120 s of equilibration
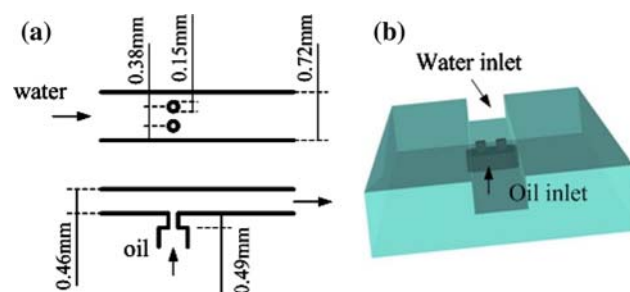

Fig. 1 The double-pore T-shaped microdevice. **a** The scales of the channel and the pores, **b** the 3-D structure of the channel

time. The average scale of the dispersed phase and the polydispersity index (σ) were determined by measuring the sizes of at least 50 droplets from recorded pictures using custom-made image-analysis software. The polydispersity index of the dispersed scale is defined by the following equation (Xu et al. 2006a):

$$\sigma = \delta / l_{av}(d_{av}) \times 100\% \tag{1}$$

where δ is the standard deviation of the length of plugs or the diameter of droplets.

3 Results and discussion

3.1 Two phase flow patterns

The two-phase flow patterns in the channel were investigated at different flow rates. Two kinds of uniform flow patterns, plugs flow and droplets flow, were successfully formed at different flow rates. The flow patterns are plotted by Fig. 2a. The plugs are defined as the discrete fluid

Fig. 2 Flow patterns in the double-pore T-shaped microchannle. **a** The flow patterns at different two-phase flow rates. **b** The micrographs illustrating the flow patterns

segments with slenderness ratios larger than 1 and the droplets are defined as the round dispersed segments. A transition state was observed between the plugs flow region and the droplet flow region. It is shows that the flow patterns in this new device are mainly determined by the phase ratios of the continuous phase to the dispersed phase. At phase ratios less than 0.3, plugs flow was observed in the channel as shown in Fig. 2bI and bII. Nearly rectangular oil plugs were formed in the channels side by side. At phase ratios between 0.3 and 0.5, a transition state was observed as shown in Fig. 2bIII. The character of the transition state is the square shape of the dispersed segments, which is different from the plugs and cannot be considered as a round droplet. At phase ratios higher than 0.5, droplets flow was formed in the channel for all the trials. Some micrographs are given in Fig. 2bIV, bV and bVI. The droplets flow in the channel side by side with short distance, and the distance increases with the increasing of the phase ratio.

The flow patterns also indicate that droplets flow can be realized easily in this new device with phase ratios (F_C/F_D) just larger than 0.5. From our previous work, higher phase ratios, ranging from 4 to 20, are commonly required to realize the droplets flow in single-pore T-shaped microchannels (Xu et al. 2006a, b, c), which limit the utilization of the T-shaped micro devices. For example in the extraction process the droplet flow can provide large interface area to enhance the mass transfer rate, but sometimes the phase ratio must be strictly controlled at a low level to obtain the separation demand. In the multiphase reactions the droplet flow can provide large interface area to enhance mass transfer rates and the reactions but the phase ratio should be fixed by the stoichiometric proportion.

A comparison of this new microdevice with the common T-shaped microchannels is listed in Table 1. The results show that the phase ratios should be at least higher than 4 to obtain droplets flow in the common single-pore microchannels and but only 0.5 is enough in the double-pore T-shaped microchannel, which expands the operating range of the droplets flow in microchannels.

3.2 Dispersion process

The formation of droplets flow at low phase ratio is a notable character of the double-pore T-shaped microdevice. Actually, this phenomenon is rooted from the special droplet formation process in the microchannel. In this section we focus on the time profile of the dispersed phase formation and discuss the characters of the microdispersed process. Figure 3 shows a series of micrographs of the plug and the droplet formation process. The droplets (plugs) form from the micro pores alternately under the
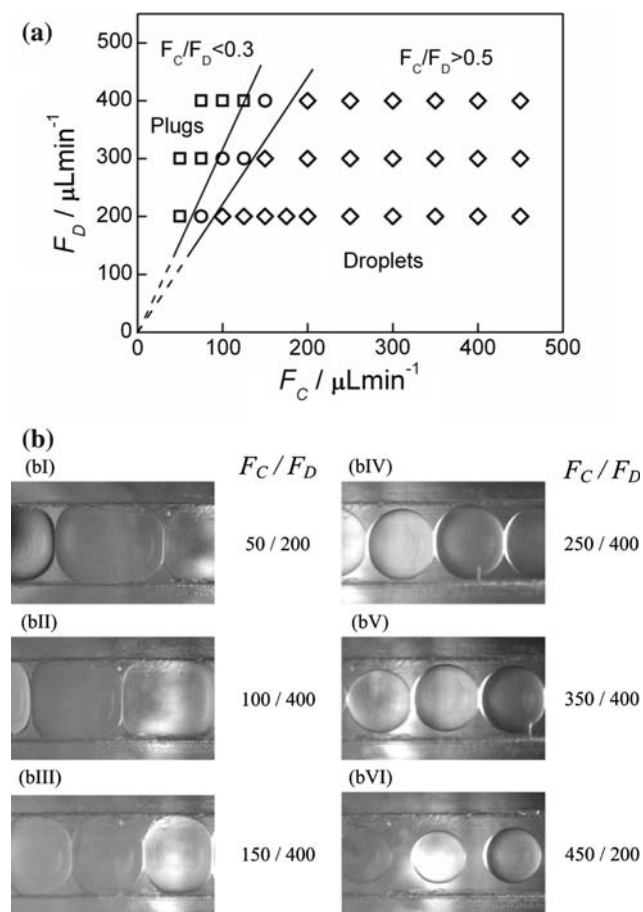
Table 1 The comparison of droplets flow in common T-shaped microchannels and in the double-pore micro-device

Devices	Dispersed method	System	Phase ratios
Common T-shaped	Crossflowing rupture	Octane/Water(SDS)	>20
	Crossflowing rupture	Water/Hexadecane(Span80)	>4
	Perpendicular shear force-inducing	Octane/Water(SDS)	>10
	Perpendicular shear force-inducing	Hexadecane/Water(SDS)	>5
Double-pore T-shaped	Crossflowing rupture	Octane/Water(SDS)	>0.5

Fig. 3 Micrographs of the plug and droplet formation process. **a** $F_C = 100$ μL/min, $F_D = 300$ μL/min. **b** $F_C = 400$ μL/min, $F_D = 200$ μL/min
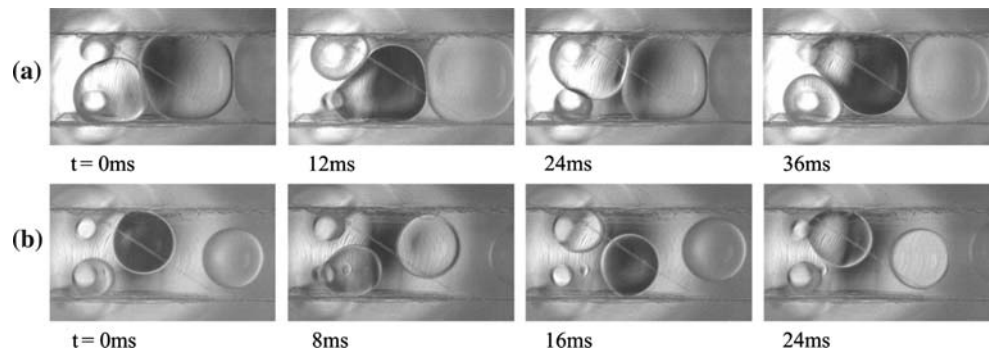
crossing flow, similar with what happens in the cross-junction channels (Zheng et al. 2004; Nisisako et al. 2008).

Another interesting thing in the dispersed process was observed in the plug formation process. The initial droplets (the plugs or droplets before rupture) on the two pores are next to each other but do not coalesce. This affects on the droplet formation process distinctly. According to Garstecki's work (Garstecki et al. 2006) the dispersed phase has a tendency to block the channel to form plugs, and long plugs was produced in their work, i.e., relative length $3 < L/w < 10$ at phase ratios less than 0.3 (L is the length of the plug and w is the width of the channel). However, in this work only short plugs ($L/w < 1.4$) was produced at these phase ratios. It is due to the existence of another force in the microchannel that accelerates the rupture process of the dispersed phase as shown in Fig. 4. Figure 4a gives an instantaneous 2-D graph of the plug formation process. A large droplet is formed on Pore **b** followed with a small partner droplet on Pore **a**. Since the initial droplets are enlarged continuously in the microchannel, a repulse exists between them, providing an additional force (F_P in the figure) on the earlier formed droplet. Together with the shearing force of the cross-flow (F_S in the figure) the plugs can be ruptured quickly in this new device.

In the droplet formation process, the initial droplets are not contacted with each other. Although the direct effect of repulse between the initial droplets does not exist, the repulse from the partner droplet cannot be neglected. During the rupturing of the big droplet, the small partner droplet is still enlarging and the draining effect from the
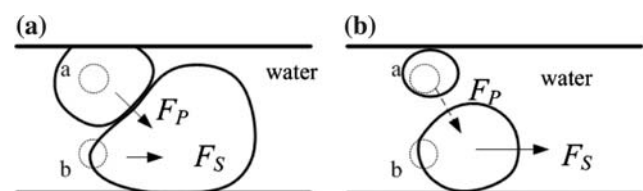

Fig. 4 The 2-D graphs of the plug formation and droplet formation. **a** Plug formation. **b** droplet formation

partner droplet gives a repulse on the big droplet as shown in Fig. 4b. Due to the additional repulse effect, the dispersed phase is ruptured quickly and has little chance to block the channel to form the plugs, thus the droplets flow can be performed in this new microdevice at low phase ratios.

Furthermore, to deeply discuss the alternate formation behavior of the droplets, an investigation was made on the impetus and the resistances of the dispersed fluid in the droplet growth process. Since the two pores are connected at both inlets and outlets, the flow distribution in the two pores abides by the rule of impetus and resistance balance. In this work the resistances mainly come from the interfacial tension pore resistance and the impetus are the pressure difference between the pressure in the inlet of the dispersed phase and the pressure in the droplet. According to Lammertink's work, (Geerken et al. 2007) the pressure difference caused by the pore resistance is approximately the sum of Hagen–Poiseuille's resistance and Sampson's resistance, which is expressed in Eq. (2).

$$\Delta p_f = R_{p,HP+S} V_D \mu_D = \left(\frac{128 l_p}{\pi d_p^4} + \frac{24}{d_p^3} \right) V_D \mu_D$$
$$= 2.5 \times 10^{10} \cdot V_D \qquad (2)$$

where l_p is the depth of the pore, d_p is the diameter of the pore, V_D is dispersed phase flow rate through a pore and μ_D is the viscosity of the dispersed phase (0.54 mPa s at 20°C). The impetus is calculated with Eq. (3)

$$\Delta p_i = P_D - (P_C + \Delta p_S) \qquad (3)$$

where P_D is the pressure in the dispersed fluid inlet and P_C is the pressure at the junction in the continuous fluid as shown in Fig. 5; Δp_s is the supplementary pressure in the micro droplet. The supplementary pressure is caused from the interfacial tension of the micro scale droplet and it can be calculated by the Young–Laplace equation with the curvature of the droplet. An assumption of spherical droplet is made in this work and the supplementary pressure can by estimated by Eq. (4).

$$\Delta p_S \sim \Delta p_{Y-L} = \frac{4\gamma}{d} \qquad (4)$$

where d is the initial droplet diameter and γ is the interfacial tension (2.53 mN m^{-1}, measured by a interfacial tension meter using a spinning drop technique, XZD-3, China).

Since the droplet diameter is changed with the enlargement of the initial droplet, the impetus is changed with time during the droplet formation process. The maximum of supplementary pressure can be estimated by the droplet diameter equal to the pore diameter $\Delta p_{S,max} \sim 4\gamma/d_p = 67.6$ Pa and the minimum can be estimated by the droplet diameter equal to the channel width $\Delta p_{S,min} \sim 4\gamma/w = 14.1$ Pa. Estimating the flow rate V_D by the average flow rate of the dispersed phase, the Δp_f is about 41 Pa at $F_D = 200$ μL/min, which is at the same level with the supplementary pressure. So it can be concluded that the interfacial tension has significant

Fig. 5 The pressure difference between the two phases in dispersion process

contribution on the flow rates distribution between the two pores.

According to the law of flowing, the pressure impetuses on the dispersed fluid is equal to the pressure difference caused by the resistances as shown in Eq. (5)

$$P_D - (P_C + \Delta p_{Y-L}) \approx \Delta p_f \qquad (5)$$

During the droplet formation process, the pressure difference between the two phases (P_D–P_C) can be seemed equally for the two pores. The small droplet bears on high Δp_{Y-L}, thus has low pore resistance. That was realized by the low flow rate from that pore, since the pore resistance is proportional to the dispersed phase flow rate (V_D). With the enlargement of the droplet, the Δp_{Y-L} decreases and the growth of initial droplet become quickly. Then the shearing force from the continuous phase exceeds the interfacial tension and the droplet is ruptured from the bottom pore. In the next period the dispersed phase repeats this growth process from a small droplet, as shown in Figs. 6 and 7. Thus, the flow rates in the two pores exhibits periodic fluctuation. This flow fluctuation produces the kinetic energy fluctuation of the dispersed phase in the droplet growth process. To have the lowest and stable energy cost of dispersion process from the two pores, the droplets formed alternately.

3.3 Effects of the flow rates on the sizes of plugs and droplets

In our previous work, it was found that the size of dispersed phase is mainly determined by the two-phase flow rates. Figure 8 shows the average length of the plugs and the average diameter of the droplets at different flow rates. In the plugs flow region the plug length decreases quickly with the increasing of the continuous phase flow rate but increases slightly with the increasing of the dispersed phase. In the droplets flow region the diameter decreases a little with the continuous phase flow rate changed from 100 to 500 μL/min and the effect of dispersed phase flow rate is slight too. These results are similar to the previous droplet formation process in common T-shaped microchannels (Xu et al. 2006a, b).

Figure 9 gives the droplet size distributions at two operating conditions and they show that the size distributions are both narrow. In this work, the polydispersity index (σ) is less than 3.5% for all the droplets flow and the polydispersity index (σ) of plugs flow is less than 6.1%.

3.4 Semi-empirical model for presenting dispersion scale

In this new device, the cross flowing ruptured technique is used to produce plugs and droplets. According to the
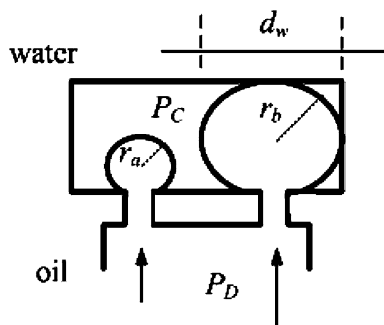
Fig. 6 Micrographs illustrating one period of the droplet formation. (F_C = 175 μL/min, F_D = 200 μL/min)
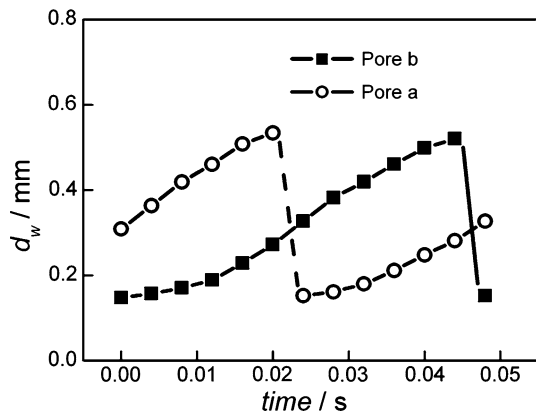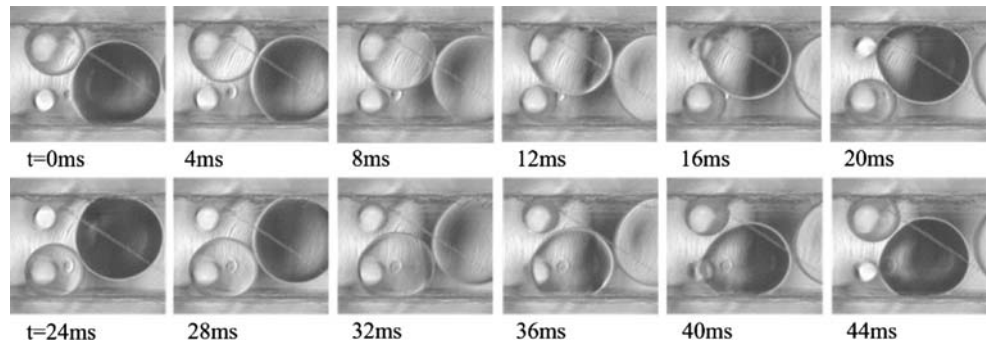
Fig. 7 The width of the initial droplets in one period. F_C = 175 μL/min, F_D = 200 μL/min)

Fig. 9 The droplet size distributions. **a** F_C = 250 μL/min F_D = 400 μL/min. **b** F_C = 400 μL/min F_D = 200 μL/min

Fig. 8 The effects of the two phases flow rates on the dispersed size

previous works (Kralj et al. 2005; Xu et al. 2006a;), how the dispersed phase is ruptured into droplets is primarily affected on the balance of shear force caused by continuous phase and the interfacial tension. A dimensionless number, Ca number, is commonly used to predict the droplet diameter. The Ca number represents the ratio of viscous force to interfacial tension:

$$Ca = \mu_C u_C / \gamma \qquad (6)$$

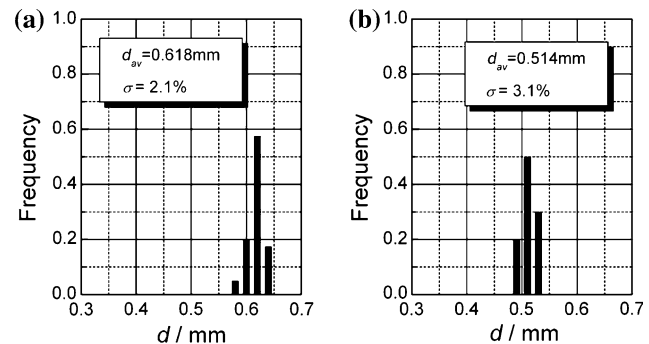where μ_C is the viscosity of continuous phase (1.005 mPa·s) and u_C is the velocity of the cross flow.

Usually, u_C is calculated by dividing the continuous phase flow rate by the sectional area of the microchannel. The effect of the repulse between the initial droplets is considered by the phase ratio in this work, since the spaces of the two phases in the channel are dependent on the hold up of two phases. Thus, the dispersion scale in this new device can be presented by the following equation:

$$\frac{l_{av}}{d_p}, \frac{d_{av}}{d_p} = k \left(\frac{F_D}{F_C} \right)^m Ca^n \qquad (7)$$

where k is a constant, m and n are the indexes of the phase ratio and the Ca number. By correlating the experimental result, we have

$$\frac{l_{av}}{d_p} = 0.47 \left(\frac{F_D}{F_C} \right)^{1/4} Ca^{-1/3} \quad (F_C/F_D < 0.3, \ Ca < 0.01)$$

$$(8)$$

for the plugs flow and

$$\frac{d_{av}}{d_p} = 1.94 \left(\frac{F_D}{F_C} \right)^{1/8} Ca^{-1/10} \quad (F_C/F_D > 0.5, Ca < 0.02)$$

$$(9)$$

for the droplets flow. The comparisons of experimental data with the correlated results are given in Fig. 10, which show the predicted results fit very well with the experimental data.
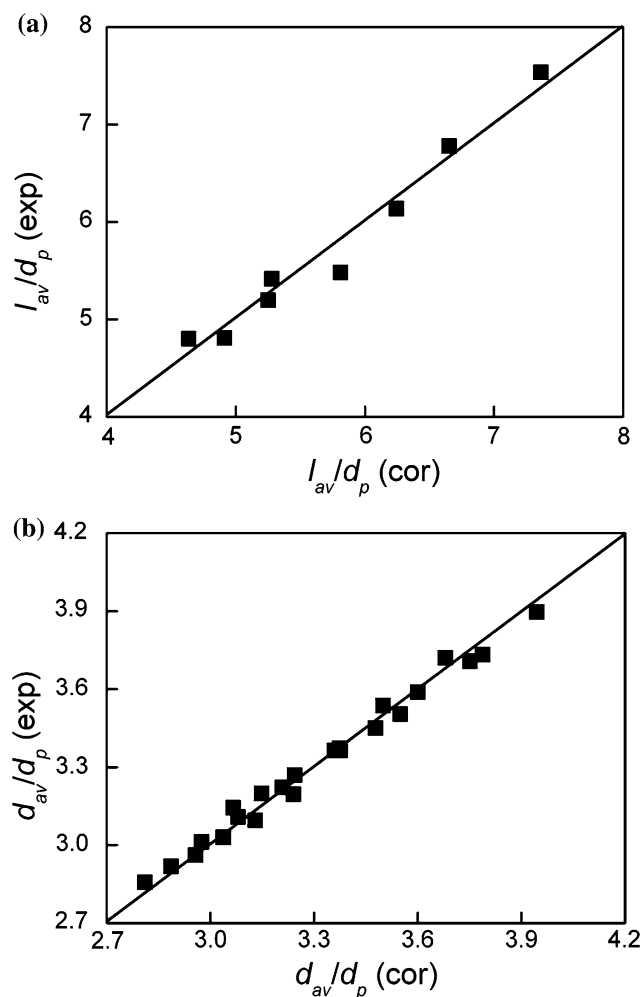
Fig. 10 Comparison of experimental data with correlated results. **a** The plugs flow ($F_C/F_D < 0.3$, $Ca < 0.01$). **b** The droplets flow ($F_C/F_D > 0.5$, $Ca < 0.02$)

4 Conclusion

This work presents a double-pore T-shaped microfluidic device, and it has been tested by the controllable preparation of mondispersed O/W emulsion with n-octane/water (SDS) system. The two-phase flow patterns were determined at different two-phase flow rates and it was found that phase ratios (F_C/F_D) just higher than 0.5 is available to obtain the droplets flow in this new device, which is much smaller than that in the common single-pore T-shaped microchannels. Only short plugs, relative length $L/w < 1.4$, were produced in this new device due to the repulsed effect between the initial droplets on the two pores. The periodic fluctuation flow in the two pores, which was demonstrated by the observed enlarging process of the initial droplets, was discussed and analyzed from the impetus and the resistance of the dispersed phase. Furthermore, the effects of the two-phase flow rates on the average plug length and

droplet diameter were investigated. It was found that the dispersed size decreased with the increasing of the continuous phase flow rate and slightly increased with the increasing of the dispersed phase. Monodispersed droplets were formed in this new device with the polydispersity index (σ) less than 3.5% for all the droplets flow. Considering the mutual effect of the initial droplets and the equilibrium between the shearing force with the interfacial tension, phase ratio and Ca number were introduced into the semi-empirical models to present the plug and droplet sizes. The correlated results fit well with the experimental data in the experimental conditions.

References

Anna SL, Bontoux N, Stoneb HA (2003) Formation of dispersions using "flow focusing" in microchannels. Appl Phys Lett 82:364–366

Chen Y, Wang YJ, Yang LM, Luo GS (2008) Micrometer-sized monodispersed silica spheres with advanced adsorption properties. AIChE J 54:298–309

Christopher GF, Anna SL (2007) Microfluidic methods for generating continuous droplet streams. J Phys D Appl Phys 40:R319–R336

Chu LY, Kim JW, Shah RK, Weitz DA (2007a) Monodisperse thermoresponsive microgels with tunable volume-phase transition kinetics. Adv Funct Mater 17:3499–3504

Chu LY, Utada AS, Shah RK, Kim JW, Weitz DA (2007b) Controllable monodisperse multiple emulsions. Angew Chem Int Ed 46:8970–8974

deMello AJ (2003) Control and detection of chemical reactions in microfluidic systems. Nature 42:394–402

Garstecki P, Fuerstman MJ, Stonec HA, Whitesides GM (2006) Formation of droplets and bubbles in a microfluidic T-junction—scaling and mechanism of break-up. Lab Chip 6:437–446

Geerken MJ, Lammertink RGH, Wessling M (2007) Interfacial aspects of water drop formation at micro-engineered orifices. J Colloid Interface Sci 312:460–469

Gong XC, Lu YC, Xiang ZY, Zhang YN, Luo GS (2007) Preparation of uniform microcapsules with silicone oil as continuous phase in a micro-dispersion process. J Microencapsul 24:767–776

Günther A, Jensen KF (2006) Multiphase microfluidics: from flow characteristics to chemical and materials synthesis. Lab Chip 6:1487–1503

Joanicot M, Ajdari A (2005) Droplet control for microfluidics. Science 309:887–888

Kobayashi I, Mukataka S, Nakajima M (2004) Effect of slot aspect ratio on droplet formation from silicon straight-through microchannels. J Colloid Interface Sci 279:277–280

Kobayashi I, Mukataka S, Nakajima M (2005) Novel asymmetric through-hole array microfabricated on a silicon plate for formulating monodisperse emulsions. Langmuir 21:7629–7632

Kobayashi I, Nakajima M, Mukataka S (2003) Preparation characteristics of oil-in-water emulsions using differently charged surfactants in straight-through microchannel emulsification. Colloid Surf A Physicochem Eng Asp 229:33–41

Kralj GH, Schmidt MA, Jensen KF (2005) Surfactant-enhanced liquid–liquid extraction in microfluidic channels with inline electric-field enhanced coalescence. Lab Chip 5:531–535

Lambrich U, Schubert H (2005) Emulsification using microporous systems. J Membr Sci 257:76–84

Nisisako T, Torii T (2008) Microfluidic large-scale integration on a chip for mass production of monodisperse droplets and particles. Lab Chip 8:287–293

Nisisako T, Torii T, Higuchi T (2002) Droplet formation in a microchannel network. Lab Chip 2:24–26

Shui LL, Eijkel JCT, van den Berg A (2007) Multiphase flow in microfluidic systems–Control and applications of droplets and interfaces. Adv Colloid Interface Sci 133:35–49

Song H, Tice JD, Ismagilov RF (2003) A microfluidic system for controlling reaction networks in time. Angew Chem Int Ed 42:767–772

Song H, Chen DL, Ismagilov RF (2006) Reactions in droplets in microfluidic channels. Angew Chem Int Ed 45:7336–7356

Sugiura S, Nakajima M, Kumazawa N, Iwamoto S, Seki M (2002a) Characterization of spontaneous transformation-based droplet formation during microchannel emulsification. J Phys Chem B 106:9405–9409

Sugiura S, Nakajima M, Seki M (2002b) Prediction of droplet diameter for microchannel emulsification. Langmuir 18:3854–3859

Tan J, Xu JH, Li SW, Luo GS (2008) Drop dispenser in a cross-junction microfluidic device: scaling and mechanism of break-up. Chem Eng J 136:306–311

Tice JD, Lyon AD, Ismagilov RF (2004) Effects of viscosity on droplet formation and mixing in microfluidic channels. Anal Chim Acta 507:73–77

van der Graaf S, Steegmans MLJ, van der Sman RGM, Schröen CGPH, Boom RM (2005) Droplet formation in a T-shaped microchannel junction: a model system for membrane emulsification. Colloid Surf A Physicochem Eng Asp 266:106–116

Wang WH, Zhang ZL, Xie YN, Wang L, Yi S, Liu K, Liu J, Pang DW, Zhao XZ (2007) Flow-focusing generation of monodisperse water droplets wrapped by ionic liquid on microfluidic chips: from plug to sphere. Langmuir 23:11924–11931

Xu JH, Li SW, Tan J, Wang YJ, Luo GS (2006a) Preparation of highly monodisperse droplet in a t-junction microfluidic device. AIChE J 52:3005–3010

Xu JH, Li SW, Tan J, Wang YJ, Luo GS, Chen GG (2006b) Controllable preparation of monodisperse O/W and W/O emulsions in the same microfluidic device. Langmuir 22:7943–7946

Xu JH, Luo GS, Li SW, Chen GG (2006c) Shear force induced monodisperse droplet formation in a microfluidic device by controlling wetting properties. Lab Chip 6:131–136

Xu QY, Nakajima M (2004) The generation of highly monodisperse droplets through the breakup of hydrodynamically focused microthread in a microfluidic device. Appl Phys Lett 85:3726–3728

Zheng B, Tice JD, Ismagilov RF (2004) Formation of droplets of alternating composition in microfluidic channels and applications to indexing of concentrations in droplet-based assays. Anal Chem 76:977–4982